

1 **In-depth phylogenomic analysis of arbuscular mycorrhizal fungi based on a comprehensive
2 set of de novo genome assemblies**

3
4 Merce Montoliu-Nerin ¹, Marisol Sánchez-García ^{1,2}, Claudia Bergin ³, Verena Esther Kutschera
5 ⁴, Hanna Johannesson ⁵, James D. Bever ⁶, Anna Rosling ^{1*}

6

7 1. Department of Ecology and Genetics, Evolutionary Biology, Uppsala University, Uppsala,
8 Sweden.

9 2. Uppsala Biocentre, Department of Forest Mycology and Plant Pathology, Swedish
10 University of Agricultural Sciences, Uppsala, Sweden

11 3. Department of Cell and Molecular Biology, Uppsala University, and Microbial Single Cell
12 Genomics Facility, Science for LifeLaboratory, Uppsala, Sweden.

13 4. Department of Biochemistry and Biophysics, National Bioinformatics Infrastructure
14 Sweden, Science for Life Laboratory, Stockholm University, Solna, Sweden.

15 5. Department of Organismal Biology, Systematic biology, Uppsala University, Uppsala,
16 Sweden.

17 6. Department of Ecology and Evolutionary Biology, and Kansas Biological Survey,
18 University of Kansas, Lawrence, Kansas, USA

19

20 *Corresponding authors: merce.montoliu@gmail.com, Anna.Rosling@ebc.uu.se

21 **Summary**

22 • Morphological characters and nuclear ribosomal DNA (rDNA) phylogenies have so far been
23 the basis of the current classifications of arbuscular mycorrhizal (AM) fungi. Improved
24 understanding of the phylogeny and evolutionary history of AM fungi requires extensive
25 ortholog sampling and analyses of genome and transcriptome data from a wide range of taxa.

26 • To circumvent the need for axenic culturing of AM fungi we gathered and combined
27 genomic data from single nuclei to generate *de novo* genome assemblies covering seven
28 families of AM fungi. Comparative analysis of the previously published *Rhizophagus*
29 *irregularis* DAOM197198 assembly confirm that our novel workflow generates high-quality
30 genome assemblies suitable for phylogenomic analysis. Predicted genes of our assemblies,
31 together with published protein sequences of AM fungi and their sister clades, were used for
32 phylogenomic analyses.

33 • Based on analyses of sets of orthologous genes, we highlight three alternative topologies
34 among families of AM fungi. In the main topology, Glomerales is polyphyletic and
35 Claroideoglomeraceae, is the basal sister group to Glomeraceae and Diversisporales.
36 • Our results support family level classification from previous phylogenetic studies. New
37 evolutionary relationships among families were highlighted with phylogenomic analysis
38 using the hitherto most extensive taxon sampling for AM fungi.

39

40 **Keywords:** Arbuscular mycorrhizal fungi, genomics, phylogenetic, single nuclei sequencing,
41 topology

42

43 2 figures in color

44 Supporting information in separate word file with 5 tables, 16 figures

45 2 supplementary data files –

46

47 Additional information in OSF: DOI 10.17605/OSF.IO/2ZYP4

48 Data in ENA (XX), and OSF: DOI 10.17605/OSF.IO/2ZYP4

49 **Introduction**

50 Arbuscular mycorrhizal (AM) fungi are an ecologically important group of fungi that form
51 ubiquitous associations with plants, establishing symbiosis with up to 80% of land plants species
52 (Parniske, 2008; Smith and Read, 2008). AM fungi play foundational roles in terrestrial
53 productivity, and there is accumulating evidence that AM fungal taxa are functionally distinct
54 and that their community composition have functional consequences for terrestrial ecosystems
55 (Hoeksema *et al.*, 2018; Koziol *et al.*, 2018). Therefore, progress in understanding the
56 ecologically distinct roles of AM fungi depends upon accurate phylogenetic inference at all
57 taxonomic levels.

58

59 Available literature identify that all AM fungi form a monophyletic lineage within the fungal
60 kingdom. This lineage is taxonomically classified either as a phylum, Glomeromycota,
61 (Schüßler, Schwarzott and Walker, 2001; James *et al.*, 2006; Hibbett *et al.*, 2007; Schüßler and
62 Walker, 2010; Tedersoo *et al.*, 2018) or as the sub-phylum Glomeromycotina, which together
63 with Mortierellomycotina and Mucoromycotina, make up the phylum Mucoromycota (Spatafora
64 *et al.*, 2016; James *et al.*, 2020, Li *et al.*, 2021). The current consensus classification of AM-
65 fungal species into genera and families was established by Redecker and co-authors in 2013,
66 when systematists with long experience in the biology and taxonomy of AM fungi joined forces

67 to integrate morphological and molecular phylogenetic evidence to generate a meaningful
68 classification that reflects evolutionary relationships (Redecker *et al.*, 2013). Molecular evidence
69 at the time was primarily based on partial sequences of nuclear ribosomal DNA (rDNA). Around
70 300 species of AM fungi are currently described and classified into 33 genera, twelve families
71 and four orders (Redecker *et al.*, 2013; Wijayawardene *et al.*, 2018).

72

73 Molecular identification of AM fungi to genera and family is usually possible based on
74 sequences of small subunit (SSU) or large subunit (LSU) regions of rDNA genes (Redecker *et*
75 *al.*, 2013, Öpik *et al.*, 2013). However, species level inference based on rDNA genes is difficult
76 due to high levels of intra species variation (Stockinger, Walker and Schüßler, 2009; House *et*
77 *al.*, 2016). While the rDNA operon is commonly found in a multi-copy tandem repeat
78 organization across fungi (Lofgren *et al.*, 2019), in AM fungi different rDNA variants can be
79 scattered across the genome (Vankuren *et al.*, 2013; Maeda *et al.*, 2018) and lack the usual
80 tandem organization (Maeda *et al.*, 2018). The fact that rDNA genes are present as paralogs in
81 AM fungal genomes (Maeda *et al.*, 2018) likely explains the high levels of within strain and
82 species diversity of rDNA sequences.

83

84 Limitations of single-locus phylogenetic inference and paralogous nature of rDNA genes in AM
85 fungi, calls for the need to generate extensive ortholog datasets from taxa representing different
86 families, in order to accurately infer phylogenetic relationships among AM fungal lineages. One
87 approach in this direction was achieved in a recent study using spore transcriptomic data for
88 phylogenomic analysis of nine taxa from seven families (Beaudet *et al.*, 2018). In the study
89 Glomerales was recovered as polyphyletic (Beaudet *et al.*, 2018), in contrast to earlier ribosomal
90 genes phylogenies where Glomerales was found to be monophyletic (Krüger *et al.*, 2012). Other
91 phylogenomic studies have not addressed relations among families largely due to limited taxon
92 sampling (Sun *et al.*, 2018; Morin *et al.*, 2019, Venice *et al.*, 2020, Li *et al.*, 2021). Due to
93 difficulties in obtaining enough pure DNA for whole genome sequencing available genomic data
94 still represent only a fraction of the diversity of AM fungi.

95

96 Progress in AM fungal genomics has been limited by their biology. AM fungi complete their life
97 cycle underground, as obligate symbionts of plant roots, and reproduce through multinuclear
98 asexual spores (Bonfante and Genre, 2010). The spores are the largest isolable structure
99 produced, but large-scale isolation of spores is needed in order to obtain enough DNA for whole
100 genome sequencing. Such large-scale harvest of spores is only possible with AM fungi grown in
101 axenic cultures where the fungus produces spores in a compartment separate from the

102 transformed plant roots that it associates with (Tisserant *et al.*, 2013), or for the rare taxa, such as
103 *Diversispora epigaea* that forms fruitbodies above ground, from which large amounts of spores
104 can be extracted (Sun *et al.*, 2018). Axenic culturing methods are time-consuming and have only
105 been successful for a handful of species (Kameoka *et al.*, 2019). Due to the difficulty of
106 producing clean cultures and isolate high quality DNA extracts for the majority of AM fungal
107 species, it has been a slow path towards genomic studies of AM fungi (Tisserant *et al.*, 2013; Lin
108 *et al.*, 2014; Chen *et al.*, 2018; Kobayashi *et al.*, 2018; Sun *et al.*, 2018; Morin *et al.*, 2019,
109 Venice *et al.*, 2020).

110

111 AM fungal hyphae and their asexual spores are coenocytic, and sequence analysis of individual
112 nuclei have been used to analyze intra organismal polymorphism mainly by mapping reads of
113 single nuclei to reference genomes of the model AM fungus *Rhizophagus irregularis* (Lin *et al.*,
114 2014; Ropars *et al.*, 2016; Chen *et al.*, 2018). To circumvent the obstacle of pure culturing, a
115 workflow was developed that takes advantage of automated nuclei sorting by extracting nuclei
116 from un-germinated spores, directly extracted from soil. Single nuclei were sorted, followed by
117 whole genome amplification (WGA) and sequencing. Finally, the data from several nuclei were
118 combined to build a *de novo* genome assembly of *Claroideoglomus claroideum* (Montoliu-Nerin
119 *et al.*, 2020). With this novel workflow AM fungal genome assemblies can be obtained from as
120 little as one single spore, independently of the species ability to grow in axenic cultures. Similar
121 approaches have been successfully applied in other organisms for which limited access to pure
122 biological material suitable for extraction of high-quality DNA has prevented genome
123 sequencing (Stepanauskas and Sieracki, 2007; Woyke *et al.*, 2009; Heywood *et al.*, 2011; Yoon
124 *et al.*, 2011; Walker *et al.*, 2014; Wideman *et al.*, 2019).

125

126 In this study, we sorted and sequenced nuclei from AM fungal spores representing species across
127 Glomeromycota, aiming to have two taxa for each genus. To evaluated the quality of assemblies
128 generated by our workflow, we included *Rh. irregularis* DAOM197198, a strain for which a
129 reference genome generated from an axenic culture is available (Chen *et al.*, 2018), and
130 compared this published assembly with our newly generated assembly. A final count of 22
131 strains, from ten genera, across seven families were successfully sequenced, and *de novo* genome
132 assemblies were constructed. Our newly generated dataset contains 18 taxa for which genome
133 data was previously not available. This comprehensive taxon sampling allowed us to infer
134 evolutionary relationships among AM fungi. Furthermore, the release of new whole genome
135 assemblies provides a resource to the research community, for those interested in further
136 exploring genetics and evolution of this important group of fungi.

137 **Material and methods**

138 Fungal strains

139 Taxa were selected to represent most families in Glomeromycota (Schüßler, & Walker, 2010;
140 Redecker et al., 2013), aiming for two species per genus (Table S1). The isolates were obtained
141 as whole inoculum from the International culture collection of (vesicular) arbuscular mycorrhizal
142 fungi (INVAM) at West Virginia University, Morgantown, WV, USA (*Acaulospora*
143 *colombiana*, *Acaulospora morrowiae*, *Ambispora gerdemannii*, *Ambispora leptoticha*,
144 *Cetraspora pellucida*, *Claroideoglomus candidum*, *Claroideoglomus claroideum*, *Dentiscutata*
145 *erythropa*, *Dentiscutata heterogama*, *Diversispora eburnea*, *Funneliformis caledonius*,
146 *Gigaspora rosea*, *Racocetra fulgida*, *Racocetra persica*, *Scutellospora calospora*, *Paraglomus*
147 *brasiliandum*, *Paraglomus occultum*), James D. Bever's lab, University of Kansas, USA
148 (*Cetraspora pellucida*, *Claroideoglomus candidum*, *Funneliformis mosseae*, *Gigaspora*
149 *margarita*), and as spores in a tube from Agriculture and Agri-food Canada, Government of
150 Canada (*Rh. irregularis* DAOM197198). In addition to the AM fungi sampled for this study, we
151 included the annotated genome assemblies of previously sequenced isolates of AM fungi (Table
152 S2). Furthermore, we included all species of the closest sister lineages with available genome
153 assemblies and annotations (December 2019) in the JGI (Joint Genome Institute) database, i.e.
154 Morteriellomycota (2 taxa, Mondo et al., 2017; Uehling et al., 2017) and Mucoromycota (12
155 taxa, Ma et al., 2009; Wang et al., 2013; Schwartze et al., 2014; Chibucos et al., 2016;
156 Corrochano et al., 2016; Mondo, Dannebaum, et al., 2017; Mondo, Lastovetsky, et al., 2017;
157 Chang et al., 2019) (Table S2). Finally, representatives of Dikarya was included as an outgroup,
158 with three representatives of Ascomycota, one taxon each from the subphyla Taphrinomycotina
159 (Pomraning et al., 2018), Saccharomycotina (Wood et al., 2002), and Pezizomycotina (Martin et
160 al., 2010); and three representatives of Basidiomycota, one taxon each from the subphyla
161 Agaricomycotina (Martin et al., 2008), Ustilaginomycotina (Kämper et al., 2006), and
162 Pucciniomycotina (Schwessinger et al., 2018) (Table S2).

163 Nuclear sorting and whole genome amplification

164 Spores were extracted from whole inoculum cultures by sieving, followed by a sucrose gradient
165 centrifugation as described in Montoliu-Nerin et al., 2020. A single spore or a pool of spores
166 (Table S1) were then rinsed and stored in 20 µl ddH₂O in a 1.5 ml tube. Spores were crushed
167 with a sterile pestle after adding 180 µl of 1x PBS and DNA was stained by adding 1 µl of 200x
168 SYBR Green I Nucleic Acid stain (InvitrogenTM, Thermo Fisher Scientific, MA, USA). The
169 nuclear sorting with flow activated cell sorter (FACS) proved to be more successful when the
170 crushed spore solution was transferred to the small 0.5 ml tube for staining. This allowed the

171 spore debris to settle while the nuclei remained in solution. The sample was left staining for 30
172 to 60 minutes, and lower sorting performance was observed when exceeding that time. The
173 nuclear sorting was performed at the SciLifeLab Microbial Single Cell Genomics Facility with a
174 MoFlo™ Astrios EQ sorter (Beckman Coulter, USA), as in Montoliu-Nerin *et al.*, 2020. Briefly,
175 a 100 μ m nozzle was used and the sheath fluid, 0.1 μ m filtered 1x PBS, was run at 25 psi. Nuclei
176 populations were identified via nuclei acid staining using the 488 nm laser and a 530/40
177 bandpass filter over forward or side scatter. Individual nuclei were deposited into 96- or 384-
178 well plates using stringent single-cell sort settings (single mode, drop envelope 1). These sort-
179 settings abort target cells if another particle of any type is in the same or the neighboring drop,
180 thereby increasing the number of aborts while ensuring that only one particle gets sorted per
181 well. Each day of sorting, the sort precision was determined with beads sorted onto a slide and
182 counted manually under the microscope. A low event rate was used to decrease the risk of
183 sorting doublets, for most samples below 500 events per second with a drop generation of
184 >40,000 per second corresponding to well below 1% of nuclei in the samples. Most of the
185 remaining particles were low in SYBR Green fluorescence. To each plate, up to 48 nuclei were
186 sorted leaving the rest of the wells empty. Plates with sorted nuclei were stored at -80°C.
187

188 DNA from the nuclei was amplified with the enzyme Phi29 with multiple displacement
189 amplification (MDA). MDA reactions were run under clean conditions using the RepliPhi kit
190 (Epicentre) in a 15 μ l reaction volume in 96-well plates or with the Repli-g Single Cell kit
191 (Qiagen) in a 10 μ l reaction volume in 384-well plates. The nucleic acid stain SYTO 13 was
192 added to the reaction to follow the DNA amplification over time. Protocol including plate size
193 and MDA kit was changed over time (Table S1, detailed sorting information is available in the
194 linked public OSF and Supplementary data file 1).

195 Sequencing of single nuclei

196 Amplified DNA of single nuclei were screened for the presence of DNA of fungal or bacterial
197 origin through PCR amplification of rDNA markers using fungal and bacterial specific primers,
198 following the protocol in Montoliu-Nerin *et al.*, 2020. Depending on the success rate of sorting
199 and MDA, a total of 7 to 24 nuclei from each isolate were sequenced independently with
200 Illumina HiSeq-X, at the SNP&SEQ Technology Platform in Uppsala at the National Genomics
201 Infrastructure (NGI) Sweden and Science for Life Laboratory, as in Montoliu-Nerin *et al.*, 2020,
202 changing to the TruSeq PCRfree DNA library preparation kit (Illumina Inc.) when enough DNA
203 was available.

204 Genome assembly and strain verification

205 Whole genome assembly was performed according to assembly workflow 3 as described in
206 Montoliu-Nerin *et al.*, 2020, in which all sets of reads from individually sequenced nuclei from
207 each strain were combined and normalized using bbnorm of BBMap v.38.08 (Bushnell, 2014),
208 setting an average depth of 100X, and then assembled using SPAdes v.3.12.0 (Bankevich *et al.*,
209 2012). We chose workflow 3 for this study as it gives a good representation and accuracy of
210 single copy genes, making it more suitable for downstream phylogenomic analyses than the
211 other two workflows tested (Montoliu-Nerin *et al.*, 2020). We used Quast v.4.5.4 (Gurevich *et*
212 *al.*, 2013) to quantitatively assess the assemblies (Table S3) and ran BUSCO v.3.0.2b (Simão *et*
213 *al.*, 2015) to assess completeness of the genome, using fungi_odb9 as lineage setting, and
214 rhizopus_oryzae as species set (Table S3-4). Raw reads and *de novo* genome assemblies are
215 deposited in ENA under the accessions xx-yy.

216

217 To verify strain identity based on a reconstructed ribosomal gene phylogeny, we extracted the
218 ribosomal gene operon from each newly assembled genome. For strains in the family
219 Claroideoglomeraceae only one of its highly diverging rDNA sequences (Vankuren *et al.*, 2013)
220 were retrieved as a complete operon. We have previously identified both rDNA variants in
221 *Claroideoglomus claroideum* using a different assembly workflow (Montoliu-Nerin *et al.*, 2020).
222 As demonstrated in that study, assembly workflow 3, which was used to produce an assembly
223 with a better representation of single copy orthologs, failed to assemble the second rDNA
224 variant. The SSU region was combined with the SSU alignment from Krüger *et al.*, (2012). The
225 whole rDNA operons extracted from the genome assemblies with verified identity, were aligned
226 and a phylogeny was reconstructed with RAxML v.8.2.10 (Stamatakis, 2014), implementing the
227 GTR model and with IQ-TREE v1.6.5 (Nguyen *et al.* 2015), using ModelFinder
228 (Kalyaanamoorthy *et al.*, 2017) and searching for the best partitioning scheme. Both analyses
229 were ran with 1000 bootstrap replicates. Extracted rDNA operons for all *de novo* genome
230 assemblies are deposited in ENA under the accessions xx-yy.

231 Genome annotation

232 Each genome assembly was annotated using a snakemake workflow (Köster and Rahmann,
233 2012) v.2.0. The workflow is publicly available at https://bitbucket.org/scilifelab-lts/genemark_fungal_annotation/ (tag v3.0), with minor updates providing the same
234 functionality. Briefly, repeats and transposable elements were *de novo* predicted in each of the
235 assemblies using RepeatModeler v1.0.8 (Smit and Hubley, 2015) and the resulting repeat library
236 was used to mask each genome assembly using RepeatMasker v4.0.7 (Smit *et al.*, 2015).
237

238 UniProt/Swiss-Prot (Bateman *et al.*, 2017) protein sequences (downloaded 8 May 2018) were
239 aligned to each of the repeat-masked genome assemblies with MAKER v3.01.1-beta (Cantarel *et*
240 *al.*, 2008). Protein coding genes were *de novo* predicted from each of the repeat-masked genome
241 assemblies with GeneMark-ES v4.33 (Ter-Hovhannisyan *et al.*, 2008), providing the genomic
242 locations of Uniprot/Swiss-Prot proteins aligned to the genome assembly to guide the gene
243 predictions. Minimum contig size to be included in self-training of the GeneMark gene
244 prediction algorithm was calculated to include at least 10Mb of training data, depending on the
245 level of fragmentation of the assembly, and was set accordingly using the parameter “--
246 min_contig” (Table of specific parameter used for each assembly is available in the linked public
247 OSF). Protein and gene names were assigned to the gene predictions using a BLASTp v2.7.1
248 (Camacho *et al.*, 2009) search of predicted protein sequences against the UniProt/Swiss-Prot
249 database with default e-value parameters (1×10^{-5}). InterProScan v5.30-69.0 (Cock *et al.*, 2013)
250 was used to collect predictive information about the predicted proteins’ functions.

251 Assessing assembly quality

252 To confirm the accuracy of our workflow we included the reference strain *Rh. irregularis*
253 DAOM197198 (Table S1) and compared the generated *de novo* genome assembly to a published
254 high-quality genome assembly DAOM197198 v.2.0 (Table S2) (Chen *et al.*, 2018). Including
255 this well characterized strain allowed us to assess the performance of our assembly workflow
256 described above. To assess efficiency and coverage of single nuclei MDA and sequencing, we
257 mapped reads from individual nuclei back to the published reference assembly and to our *de*
258 *novo* assembly of *Rh. irregularis* DAOM197198, using BWA 0.7.15 (Li and Durbin, 2009), and
259 measured both % of reads mapping and % of assembly covered with mapped reads using
260 Qualimap 2.2.1 (Okonechnikov, Conesa and García-Alcalde, 2016) and bamtools 2.3.0 stats
261 (Barnett *et al.*, 2011). We also tested for polymorphism introduced during MDA by pair-wise
262 alignment of the 271 BUSCO genes retrieved from both assemblies of *Rh. irregularis*
263 DAOM197198 using MAFFT 7.407 (Katoh and Standley, 2013) Percent similarity for the
264 alignments was calculated with esl-alistat in HMMer 3.2.1 (Hancock *et al.*, 2004). Finally,
265 orthogroups were identified with OrthoFinder 2.4.0 (Emms and Kelly, 2018) using standard
266 settings.

267 Phylogenomic analyses

268 Phylogenomic analyses were performed at different taxonomic scales, using datasets with
269 different taxon sampling (Table S2-S3). For each set of taxa, single copy orthologs (SCOs) were
270 identified from the gene predictions using OrthoMCL v.2.0.9 (Li *et al.*, 2003) using default
271 parameters. SCOs present in >50% or 100% of the taxa were selected. Amino acid sequences

were aligned using MAFFT v.7.407 (Katoh and Standley, 2013). Poorly aligned regions were removed using trimAl v.1.4.1 (Capella-Gutiérrez *et al.*, 2009) with a gap threshold of 0.1 (0.2 in the dataset with only 15 taxa selected, Table S4). Individual SCO alignments were removed if shorter than 100 amino acids. SCO alignments were used either separately, to produce individual gene trees, or concatenated, to produce maximum likelihood (ML) consensus trees. Individual SCO alignments were concatenated into a supermatrix using the script geneStitcher.py (Schluter, 2016), which also produces a partition file, with one partition per gene. Lists of SCOs used for phylogenomic inferences for each set of taxa and their corresponding gene annotations are available in the public OSF repository.

Phylogenomic inferences based on the concatenated sets of SCOs were performed using two maximum likelihood (ML) methods. All ML phylogenies were inferred using RAxML v.8.2.10 (Stamatakis, 2014), with 100 bootstrap replicates, and with a partitioned model that treated each SCO as a separate partition and implementing the PROTOGAMMAWAG model for all partitions. Secondly, ModelFinder (Kalyaanamoorthy *et al.*, 2017) was run for every partition, and a consensus ML tree was generated with 100 bootstrap replicates in IQ-TREE v.1.6.5 (Nguyen *et al.*, 2015). Topologies and support values from both ML inference methods were highly comparable, therefore, we only present the RAxML topologies but adding also support values from the IQ-TREE analysis. In the dataset that included available spore transcriptomic data (Beaudet *et al.*, 2018, Table S2), only 17 SCOs were shared among >50% of the taxa and a phylogeny was inferred merely for visualization purposes using RAxML as described above with the concatenated alignment of retrieved SCOs.

We also reconstructed phylogenies avoiding the use of concatenated alignments for the datasets including taxa in Glomeromycota, and its sister clades (Mortierellomycota and Mucoromycota). Individual gene trees were inferred using RAxML and IQ-TREE, both with 100 bootstrap replicates. A coalescent-based species tree was inferred with ASTRAL-II using multi-locus bootstrapping (Mirarab and Warnow, 2015). Furthermore, a Bayesian phylogeny was inferred this dataset using Phylobayes (Lartillot, Lepage and Blanquart, 2009), under the site-heterogeneous CAT+GTR+G4 model on a total alignment of 144,177 amino acids. Two chains were run of ~200k and ~120k generations respectively and full convergence was achieved. For in-depth analysis of topologies within Glomeromycota, three additional analyses were performed. A dataset containing all Glomeromycota taxa was used to produce a splits network in IQ-TREE v.1.6.5 (Nguyen *et al.*, 2015) with the command iqtree --net, the tree was then visualized in SplitsTree5 (Huson and Bryant, 2006) with a maximum dimension of 2. To

307 increase robustness, further analyses were performed using a set of only 15 selected taxa,
308 representing the assemblies with highest N50 and BUSCO-estimated completeness (Table S3-4),
309 which resulted in a comprehensive dataset of 799 SCOs shared among all taxa (as opposed to 31
310 SCOs when including all Glomeromycota taxa). In order to visualize all topologies branching
311 over the tree landscape, the previously inferred individual gene trees from RAxML and IQ-
312 TREE were used to analyze the spectra of topologies with Densitree v.2.01. Finally, we used
313 TWISST (Martin and Van Belleghem, 2017) as a topology weighting method to quantify the
314 phylogenetic relationships between the Glomeromycota families. The method is designed for
315 population genomic data and was thus adapted for our analysis. We used the individual gene
316 trees from SCOs and their bootstrap values to assess the range of different topologies supported
317 for each SCO. For visualization purposes, the concatenated set of SCOs was input as an artificial
318 chromosome, across which we visualized the dominant topology, of three possible topologies,
319 for each SCO.

320 **Results**

321 Presenting 21 *de novo* genome assemblies of AM fungi

322 Using our novel workflow for *de novo* assembly of genomes by combining single nuclei
323 sequence data (Montoliu-Nerin *et al.*, 2020), we attempted to sequence 31 AM fungal isolates,
324 representing eight families with at least two taxa from each of 15 genera (Table S1). Spores from
325 all 31 isolates were extracted for nuclei sorting and DNA amplification. For two of the taxa,
326 *Ar. trappei* and *E. infrequency*, we failed to sort nuclei, and these were thus omitted from the
327 method pipeline. After whole genome amplification with MDA on the sorted nuclei, samples
328 from the remaining 29 isolates were screened for presence of DNA of fungal and bacterial origin
329 by PCR amplification of rDNA sequences. Fungal DNA was successfully amplified from 25 of
330 the isolates, while samples from four isolates did not and *Se. constrictum*, *Gl. microaggregatum*,
331 *Gl. gold*, and a second isolate of *E. infrequency* were thus excluded from sequencing (Table S1).

332
333 After Illumina sequencing of separate amplified nuclei from the AM fungal isolates we
334 generated *de novo* genome assemblies following the method presented as assembly workflow 3
335 in Montoliu-Nerin *et al.*, (2020), where all reads were combined for each strain, normalized and
336 then assembled using SPAdes. Genome assemblies ranged from 50 to 493 Mb in size, with
337 numbers of gene predictions ranging from 11,400 to 46,500 (Table S3).

338

339 Based on the comparison of *Rh. irregularis* DAOM197198 genome assemblies, we found that
340 single nuclei MDA and sequencing were highly accurate and efficient in our workflow. On
341 average, around 99% of the reads mapped to both our *de novo* genome assembly and the
342 published reference genome v.2.0 for *Rh. irregularis* DAOM197198 (Table S5). Reads from
343 individual nuclei covered on average 50% of both assemblies (Table S5). Together these results
344 demonstrate that reads from single amplified and sequenced nuclei fully match the published
345 reference and that the whole genome is represented among the reads. Pair-wise alignment of the
346 271 BUSCO genes retrieved in both assemblies demonstrate high consistency with an average
347 similarity of 99.7% across nucleotide alignments. Of the 271 pairwise aligned BUSCO genes, a
348 total of 260 were identical between the two assemblies, corresponding to 96% of the retrieved
349 BUSCO genes. However, only 60% similarity was detected in one of the 271 pairwise
350 alignments, and ten alignments ranged in similarity between 84 and 99% (Supplementary
351 datafile 2). High similarity in pairwise alignments of BUSCO genes retrieved from the two
352 assemblies demonstrates that random errors possibly introduced during MDA are not retained to
353 a large extent in the assembled genome when reads from single nuclei are combined and
354 normalized before assembling with SPAdes. In our assembly of *Rh. irregularis* DAOM197198,
355 23,258 genes were predicted (Table S3) compared to 26,183 genes predicted in the published
356 assembly of *Rh. irregularis* DAOM197198 v.2.0. (Chen *et al.*, 2018). We demonstrate that our
357 *de novo* genome assembly for *Rh. irregularis* DAOM197198 contained a largely overlapping set
358 of genes in orthogroups present in the published *Rh. irregularis* DAOM197198 reference
359 genome v.2.0. Across the two genome assemblies of the same strain, a total of 13,908
360 orthogroups were identified including 88% of all predicted genes across the two assemblies, of
361 these, 94% were shared between the two genome assemblies (Table S6). Interestingly, both
362 genome assemblies contain orthogroups not recovered in the other, 403 unique to v.2.0 and 380
363 unique to our *de novo* assembly (Table S6).

364 Isolate identification in rDNA-based phylogeny

365 The complete rDNA operon, including SSU, ITS1, 5,8s, ITS2, and LSU regions was extracted
366 from the 25 newly generated genome assemblies. To confirm genus level identity of the 25
367 isolates for which we generated genome assemblies in this study, the SSU rDNA region was
368 extracted and placed into the Glomeromycota phylogeny of Krüger *et al.*, 2012 (Fig. S1). The
369 phylogenetic placement revealed that five isolates were originally misidentified. Four of these
370 were removed and one re-identified for further analysis. First, the isolate *Rh. intraradices*
371 FL208A clustered within the genus *Funneliformis* (Fig. S1), more specifically, as *F. mosseae*.
372 Morphological examination of this strain was consistent with its original identification as

373 *Rh. intraradices*. Because we could not verify that spores with the correct morphology had been
374 extracted, the genome assembly was excluded from further analyses. The isolate *F. caledonius*
375 UK203 was also identified as *F. mosseae* (Fig. S1), but kept for further analyses, since the genus
376 placement remained correct. The isolate *Diversispora epigaea* AZ150B was phylogenetically
377 misplaced based on its rDNA SSU sequence (Fig. S1), and the assembly had higher GC content
378 than the rest of isolates (Table S3), probably due to bacterial contamination. We thus decided to
379 discard this assembly since the publicly available genome assembly of *Di. epigaea* (Sun *et al.*,
380 2018) was included in the analyses. Finally, the isolates *Ar. scheckii* CL383 and *Se. viscosum*
381 MD215 were placed in the Paraglomeraceae family (Fig. S1), and subsequently eliminated from
382 further analyses, as two *Paraglomus* isolates were already included. After this confirmation step,
383 novel genome assemblies representing 21 isolates were kept for the phylogenomic analyses. A
384 phylogenetic analysis of the entire extracted rDNA operon of the 21 isolates (Fig. S2) confirmed
385 the expected topology found in previous analysis based on rDNA genes (Redecker *et al.*, 2013).

386 Phylogenomic analysis of Glomeromycota

387 Single copy orthologs shared among the 21 *de novo* genome assemblies, previously published
388 genome assemblies of AM fungi and selected outgroup taxa were identified from the predicted
389 genes and transcriptomes (Table S2-3). Published transcriptomic data from ten genera of AM
390 fungi represented by one species each (Beaudet *et al.*, 2018) is consistently placed to genus level
391 in a phylogenetic analysis with genomic data from this and previous studies (Fig. S3). However,
392 when combining genomic data with transcriptomic data, only 17 SCOs were shared among 50%
393 of the taxa, thus and published transcriptomic data was thus excluded from further analysis
394 without losing taxonomic breadth, but allowing us to work with a more comprehensive set of
395 genes.

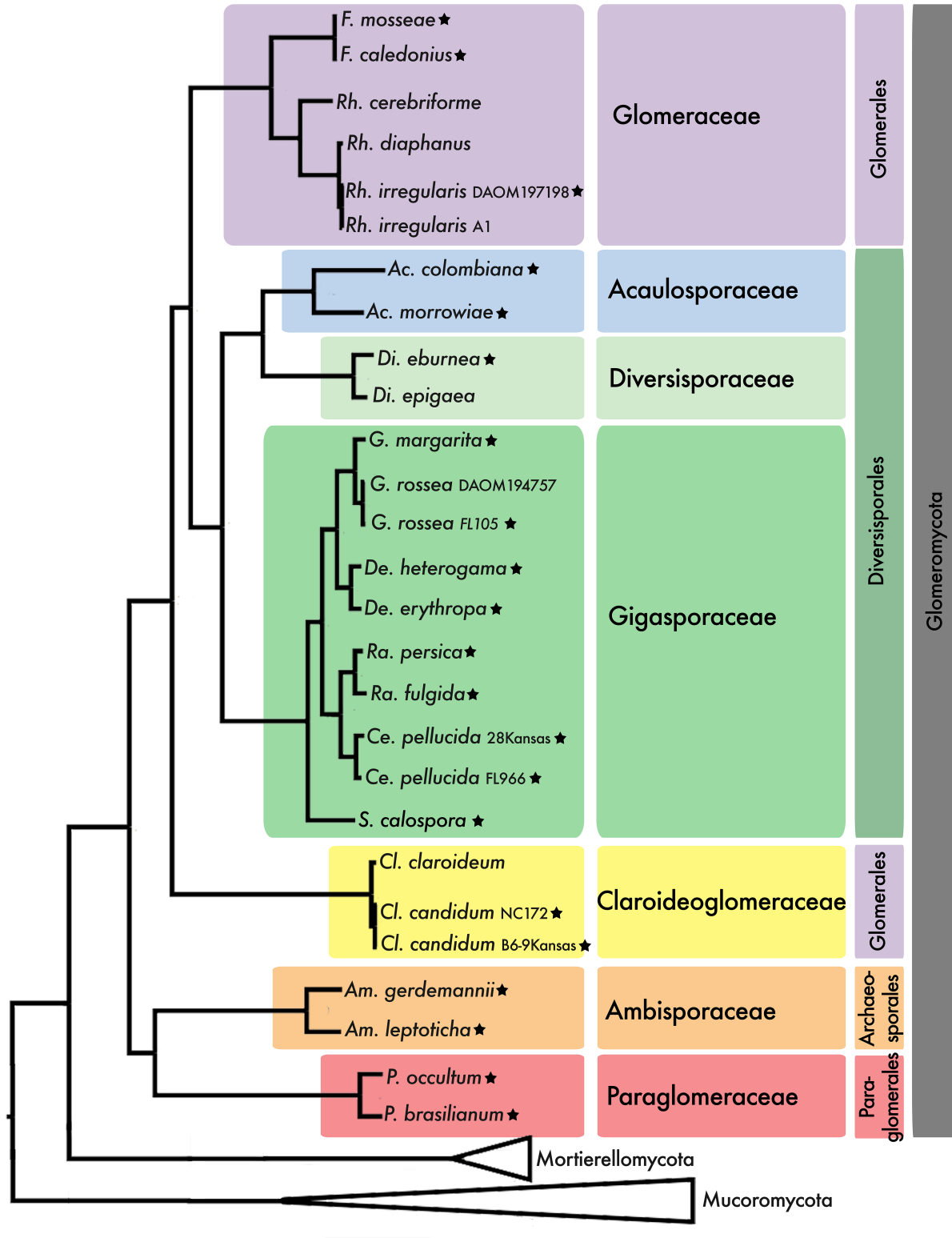
396

397 To place Glomeromycota in relation to its sister phyla, phylogenetic trees (Fig. S4-5) were built
398 using 178 SCOs identified from the gene annotations and shared among 50% of the taxa
399 included. The concatenated alignment had a length of 76,737 amino acids. Glomeromycota
400 forms a well-supported monophyletic clade (100% bootstrap support), but the relationships
401 between Morteriellomycota and Mucoromycota are not well resolved. Morteriellomycota is
402 recovered as a sister clade of Glomeromycota, with bootstrap supports of 80% in the RaxML
403 phylogeny (Fig. S5a). In the IQ-TREE phylogeny on the other hand, Morteriellomycota and
404 Mucoromycota form a well-supported sister lineage to Glomeromycota (Fig. S5b). Their internal
405 relation, however, is not well-supported in this analysis with only 43% bootstrap support for the

406 separation of Mortierellomycota and Mucoromycota (Fig. S5b). The relationships among the
407 three sister phyla thus remains unresolved in our analysis.

408

409 For in depth phylogenomic analysis of Glomeromycota, we included representatives from
410 Mortierellomycota as sister clade, and the Mucoromycota as outgroup. A concatenated
411 alignment of 371 SCOs shared among at least 50% of the taxa, gave a total alignment of 144,177
412 amino acids. All represented Glomeromycota families form well-supported monophyletic
413 lineages in the consensus species tree (Fig. 1, Fig. S6), strongly supporting available
414 phylogenetic inferences based on a combination of morphology and rDNA gene phylogenies
415 (Redecker *et al.* 2013). We found, however, that the order Glomerales is polyphyletic, with taxa
416 in Glomeraceae recovered as a sister clade to the order Diversisporales, while the family
417 Claroideoglomeraceae forms a basal sister clade to the two, with a bootstrap support of 100%
418 (Fig. 1, S6). In an ASTRAL reconstruction based on 371 ML individual gene trees, we observe a
419 low multi-bootstrapping support for the node that includes Glomeraceae and Diversisporales,
420 with a bootstrap support of 81% and 94% when using individual trees inferred with RAxML and
421 IQ-TREE, respectively (Fig. S7).



422

423 *Figure 1.* Best maximum likelihood tree inferred with RAxML from a concatenated alignment of
 424 371 single copy orthologs shared among at least 50% of the taxa. The same topology was
 425 recovered using IQ-TREE and Bayesian inference. All nodes have a bootstrap support value of
 426 100 in both analyses, and posterior probabilities of 1. Mucoromycota was used as outgroup.
 427 Stars following the taxon name mark newly sequenced strains from this study. Current
 428 taxonomic assignment based on Redecker *et al.*, 2013 is color coded, at the levels of family and

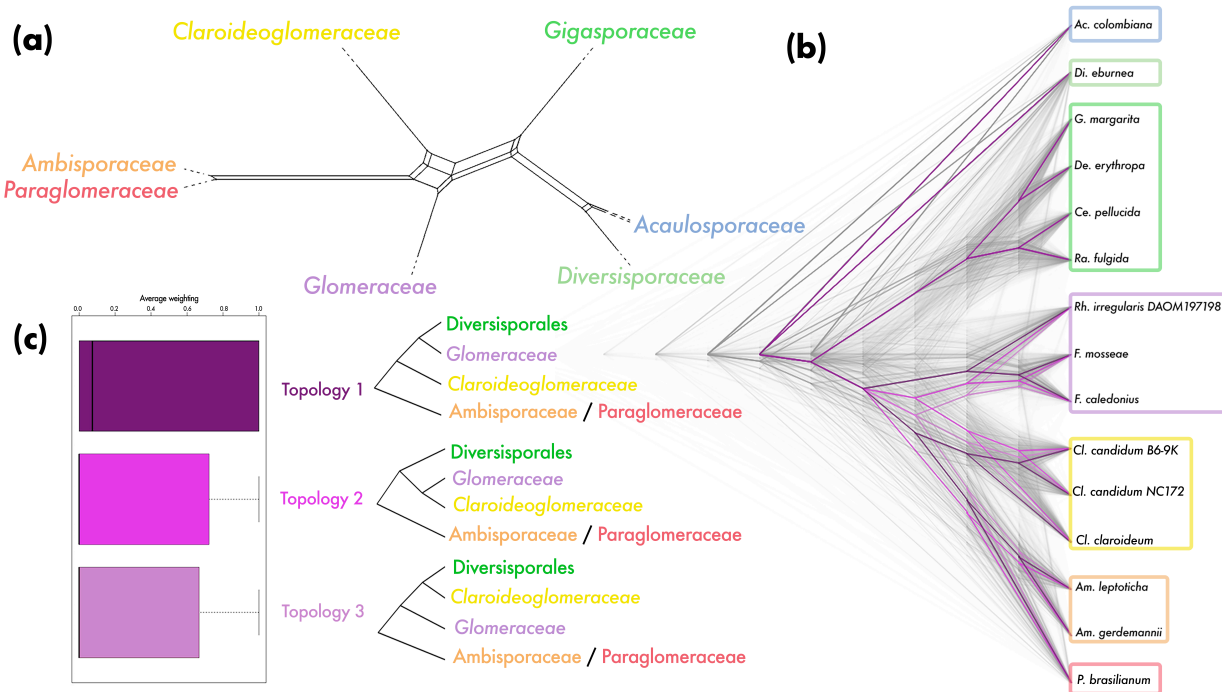
429 order. Strain identifiers are included in the taxa label when more than one node has the same
430 species name. See expanded tree in Fig. S6.

431 Exploring conflicting topologies

432 To study the relationships within Glomeromycota in more detail, different datasets were
433 produced to visualize the conflicting topologies. For this, we included only taxa within
434 Glomeromycota to generate three datasets. First, a set of 31 SCOs shared among all
435 Glomeromycota taxa included in this study, was concatenated to represent a total alignment of
436 15,443 amino acids. A second set of 1,737 SCOs represented within at least 50% of all
437 Glomeromycota taxa included in this study (Table S2-S3), represented a total alignment of
438 702,801 amino acids. Finally, we produced a dataset with a reduced selection of taxa, covering
439 all families, by picking the 15 *de novo* assembled Glomeromycota genomes with the highest
440 quality (Table S3-4). This last dataset was used to obtain a greater number of SCOs shared
441 among all analyzed taxa, with a total of 799 SCOs shared among all 15 represented taxa,
442 resulting in a total alignment of 476,329 amino acids.

443

444 The main topology of the species trees (Fig. 1, S6) was not recovered in the dataset with 31
445 SCOs shared among all Glomeromycota (Fig. S8) where instead an alternative topology with
446 Claroideoglomeraceae as a sister group of Diversiporales was inferred. This topology however
447 had low bootstrap support at 52% and 59%, in RAxML and IQ-TREE respectively (Fig. S8).
448 However, both the best ML and ASTRAL reconstruction trees, recovered the main topology
449 (Fig. 1), when using the two other Glomeromycota datasets with the highest number of SCOs
450 included, (Fig. S9-S12). Further analyses were performed using these more comprehensive
451 datasets, with 1,737 SCOs shared among 50% of the Glomeromycota taxa, and 799 SCOs shared
452 among all 15 selected Glomeromycota taxa. A Phylogenomic network reveals a clear reticulation
453 at the base of the tree, leaving the early evolutionary relationships unresolved (Fig. 2a, S13-S14).
454 The three most commonly observed topologies were visualized in one image using Densitree
455 (Bouckaert and Heled, 2014), in which all trees are stacked on top of each other (Fig. 2b, S15).
456 We find the same three topologies when using topology weighting by iterative sampling of sub-
457 trees with TWISST (Martin and Van Belleghem, 2017, Fig. 2c, S16). This analysis shows that
458 most genes support a predominant topology, in which we recovered Glomeraceae as sister of
459 Diversiporales, followed by a second topology in which Glomerales is recovered as a
460 monophyletic clade, and a third topology, in which Claroideoglomeraceae is inferred as a sister
461 group of Diversiporales (Fig. 2b-2c, S15-S16).



462

463 *Figure 2. Exploring the diversity of topologies within Glomeromycota. (a). IQ-TREE network*
464 *analysis visualized in SplitsTree5 with maximum dimension splits filter of 2, using the dataset*
465 *containing all Glomeromycota taxa, and 1,737 SCOs shared among, at least 50% of the taxa. See*
466 *Fig. S13 for expanded network with branch lengths. (b). Densitree of Glomeromycota, formed*
467 *from stacking of 799 individual gene trees and their corresponding bootstrapping trees for each*
468 *gene tree, based on selection of 15 taxa. Three main topologies are colored in three different*
469 *hues of purple, from the most common being the darkest, to the least common the lightest. For a*
470 *better visualization of topology 3, the order of taxa has been rearranged in Fig. S15. (c).*
471 *TWISST analysis of 15 taxa of Glomeromycota, grouped in four monophyletic lineages*
472 *representing the order Diversisporales, and families Glomeraceae, Claroideoglomeraceae, with*
473 *Ambisporaceae / Paraglomeraceae as an outgroup. The analysis produces a topology average*
474 *weighting of the three possible topologies (same colors as in (b)), using the 799 individual gene*
475 *trees and their corresponding bootstrapping trees. Expanded TWISST analysis in S16.*

476 **Discussion**

477 Glomeromycota encompass all known AM fungi with their characteristic life cycle involving an
478 obligate association with plants (Bonfante & Venice 2020) as well as the exceptional fungal taxa
479 *Geosiphon pyriformis* which forms a mutualistic symbiosis with the cyanobacteria *Nostoc*
480 *punctiforme* (Malar *et al.*, 2021). In the current study we present a four-fold increase in the
481 number of AM fungal genomes available, which was achieved thanks to the development of a

482 workflow for genome assembly from multiple individually amplified and sequenced nuclei
483 (Montoliu-Nerin *et al.*, 2020).

484

485 The current workflow for generating *de novo* reference genomes of AM fungi was developed by
486 our team to circumvent the need for culturing AM fungi for genomic studies (Montoliu-Nerin *et*
487 *al.*, 2020). Read mapping of data from 24 individually amplified and sequenced *Rh. irregularis*
488 DAOM197198 nuclei demonstrates near complete coverage of the published *Rh. irregularis*
489 DAOM197198 v.2.0 reference genome (Table S5), suggesting that separate amplification of
490 multiple nuclei compensates for uneven amplification of individual nuclei. Consistent recovery
491 of orthogroups in our *de novo* genome assembly of *Rh. irregularis* DAOM197198 (Table S6)
492 and evidence that mostly identical BUSCO genes are recovered from both assemblies provides
493 further support that the presented workflow generates gene sequence data suitable for
494 phylogenomic analysis. We anticipate that the release of these novel genome assemblies will
495 become an important resource for the future study of AM fungi, supplementing the previous AM
496 fungal genomes (Tisserant *et al.*, 2013; Lin *et al.*, 2014; Chen *et al.*, 2018; Kobayashi *et al.*,
497 2018; Sun *et al.*, 2018; Morin *et al.*, 2019; Montoliu-Nerin *et al.*, 2020).

498

499 Based on the most comprehensive taxon sampling thus far we present a well-supported species
500 tree for AM fungi. We find that the seven family level lineages included in the analysis represent
501 well supported monophyletic lineages. While the order Diversisporales, including three families,
502 was recovered as monophyletic we found that the order Glomerales with the two families
503 Glomeraceae and Claroideoglomeraceae was not. Comprehensive phylogenetic studies with
504 wide taxon sampling representing AM fungi have thus far mostly used rDNA sequences from
505 trap cultures (Redecker *et al.*, 2013) and environmental samples (Krüger *et al.*, 2012) and
506 recover Glomerales as monophyletic based on these markers. Similarly, our phylogenetic
507 reconstructions using only the extracted rDNA operon from the *de novo* assembled genomes
508 support Glomerales as monophyletic (Fig S2). Glomerales was previously found to be
509 polyphyletic in a phylogenomic analyses using spore transcriptomic data from nine AM fungal
510 species, where *Claroideoglomus* was recovered as a well-supported clade with Ambisporaceae
511 and Paraglomeraceae (Beaudet *et al.*, 2018). In contrast to Beaudet *et al.* (2018), we recovered
512 Glomeraceae as a sister group of Diversisporales with Claroideoglomeraceae being the basal
513 sister group of the two (Fig. 1-2). Previous phylogenomic studies using whole genomic data had
514 not yet observed this topology due to limited taxon sampling (Morin *et al.*, 2019). Further, the
515 relation of Glomeromycota to its to closest sister lineages, Mucoromycota and
516 Mortierellomycota, have not yet been resolved with strong support, and based on available data

517 the relation is best described as a polytomy (Li *et al.*, 2021). Interestingly, with the addition of a
518 considerable number of AM fungal genomes presented in this study, we recover yet a new
519 topology among the three sister lineages (Fig. S4-5). This further highlights the need for
520 increased taxon sampling in the sister lineages, particularly in Morterellomycota.
521

522 The placement of Glomeraceae as a sister group of Diversisporales is well supported in the
523 species tree (Fig. 1), but alternative topologies were indicated by the lower support based on
524 coalescence methods (Fig. S7). A more detailed analysis of the different topologies was possible
525 based on the single gene trees from orthologs shared among the included Glomeromycota taxa,
526 after removing taxa belonging to Morterellomycota and Mucoromycota, in order to have a
527 larger pool of SCOs (Fig. 2, S8-S16). The most common topology groups Glomeraceae and
528 Diversisporales, as in the species tree; a second one, which recovers Glomerales as
529 monophyletic; and a third places Claroideoglomeraceae as a sister group of Diversisporales (Fig.
530 2, S15-S16).

531 It is possible that the tree topology discordances are due to incomplete lineage sorting (Maddison
532 and Knowles, 2006), caused by long coalescence times which complicates the assessment of an
533 accurate evolutionary history. Different topologies could also result from gene flow among AM
534 fungal lineages. Documented gene family expansions correlated with genome size in AM fungi
535 (Tang *et al.*, 2016), could distort phylogenetic histories since gene expansions and contractions
536 can cause misidentification of SCOs, resulting in alignments between paralogs present as single
537 copy with different evolutionary origins and histories. A better understanding on how variation
538 in gene content and copy number variation influenced the different topologies could be achieved
539 with a deeper phylogenetic study into the whole repertoire of paralogs, moving one step further
540 from SCOs, which would also allow us to look more closely into the possible correlation
541 between gene function and the different evolutionary histories.

542 Conclusion

543 In the current study we present a considerable increase in the number of AM fungal genome
544 assemblies available, thanks to the development of single nuclei sequencing and *de novo*
545 assembling in AM fungi. We conclude that our *de novo* genome assemblies provide a
546 satisfactory representation of the genome content. While the assemblies generated with our
547 workflow are fragmented, we demonstrate that genome content is well recovered across nuclei,
548 despite variation in sequencing depth due to MDA. Further, we demonstrate that gene content is
549 soundly recovered in the *de novo* genome assemblies. We present a phylogenomic analysis of

550 AM fungi based on the most comprehensive taxon sampling across Glomeromycota to date. Our
551 results support current family-level classification and in the first and most broadly supported tree
552 topology, the order Glomerales is polyphyletic, with the family Glomeraceae being recovered as
553 a sister group to the order Diversisporales, while Claroideoglomeraceae is recovered as an
554 outgroup of the two. The new genome data presented cover seven families of the phylum
555 Glomeromycota and are expected to be a valuable contribution to the AM fungal research
556 community.

557 **Acknowledgments**

558 Funding for this project was provided by ERC (678792). We thank Y. Strid for assistance in the
559 lab and J. Morton and W. Wheeler at INVAM culture collection. Nuclei sorting and whole
560 genome amplification was done at the SciLifeLab Microbial Single Cell Genomics Facility at
561 Uppsala University. Sequencing was performed by the SNP&SEQ Technology Platform at NGI
562 Sweden and SciLife Laboratory, Uppsala, supported by the VR and the KAW. Computational
563 analyses were performed on resources provided by SNIC through UPPMAX. VK was financially
564 supported by the Knut and Alice Wallenberg Foundation as part of the National Bioinformatics
565 Infrastructure Sweden at SciLifeLab. Open access funding provided by Uppsala University. The
566 paper was greatly improved thank to comments from three anonymous reviewers.

567 **Author contribution**

568 M.M.N. initiated the project together with A.R. and J.D.B. and developed the analysis together
569 with M.S.G. and H.J.. C.B. did the nuclei sorting and whole genome amplification. M.M.N.
570 performed the bioinformatic analyses together with M.S.G., V.K. developed the annotation
571 workflow which was ran by M.M.N and M.S.G.. M.M.N. wrote the manuscript with A.R. and
572 H.J., with input from all the authors.

573 **References**

574 Bankevich, A. *et al.* (2012) ‘SPAdes: A New Genome Assembly Algorithm and Its Applications
575 to Single-Cell Sequencing’, *Journal of Computational Biology*. doi: 10.1089/cmb.2012.0021.

576 Barnett, D. W. *et al.* (2011) ‘Bamtools: A C++ API and toolkit for analyzing and managing
577 BAM files’, *Bioinformatics*. doi: 10.1093/bioinformatics/btr174.

578 Bateman, A. *et al.* (2017) ‘UniProt: The universal protein knowledgebase’, *Nucleic Acids
579 Research*. doi: 10.1093/nar/gkw1099.

580 Beaudet, D. *et al.* (2018) ‘Ultra-low input transcriptomics reveal the spore functional content and

581 phylogenetic affiliations of poorly studied arbuscular mycorrhizal fungi', *DNA Research*. doi:
582 10.1093/dnare/dsx051.

583 Bonfante, P. and Genre, A. (2010) 'Mechanisms underlying beneficial plant-fungus interactions
584 in mycorrhizal symbiosis.', *Nature communications*. Nature Publishing Group, 1(4), p. 48. doi:
585 10.1038/ncomms1046.

586 Bonfante, P. and Venice, F. (2020) 'Mucoromycota: going to the roots of plant-interacting
587 fungi', *Fungal Biology Reviews*. doi: 10.1016/j.fbr.2019.12.003.

588 Bouckaert, R. and Heled, J. (2014) *DensiTree 2: Seeing trees through the forest*, *bioRxiv -*
589 *Preprint Server*. doi: 10.1101/012401.

590 Bushnell, B. (2014) *BBMap short read aligner*, *Joint Genome Institute, department of energy*.
591 doi: 10.1016/j.avsg.2010.03.022.

592 Camacho, C. *et al.* (2009) 'BLAST+: Architecture and applications', *BMC Bioinformatics*. doi:
593 10.1186/1471-2105-10-421.

594 Cantarel, B. L. *et al.* (2008) 'MAKER: An easy-to-use annotation pipeline designed for
595 emerging model organism genomes', *Genome Research*. doi: 10.1101/gr.6743907.

596 Capella-Gutiérrez, S., Silla-Martínez, J. M. and Gabaldón, T. (2009) 'trimAl: A tool for
597 automated alignment trimming in large-scale phylogenetic analyses', *Bioinformatics*. doi:
598 10.1093/bioinformatics/btp348.

599 Chang, Y. *et al.* (2019) 'Phylogenomics of Endogonaceae and evolution of mycorrhizas within
600 Mucoromycota', *New Phytologist*. doi: 10.1111/nph.15613.

601 Chen, E. C. H. *et al.* (2018) 'High intraspecific genome diversity in the model arbuscular
602 mycorrhizal symbiont Rhizophagus irregularis', *New Phytologist*. doi: 10.1111/nph.14989.

603 Chibucos, M. C. *et al.* (2016) 'An integrated genomic and transcriptomic survey of
604 mucormycosis-causing fungi', *Nature Communications*. doi: 10.1038/ncomms12218.

605 Cock, P. J. A. *et al.* (2013) 'Galaxy tools and workflows for sequence analysis with applications
606 in molecular plant pathology', *PeerJ*. doi: 10.7717/peerj.167.

607 Corrochano, L. M. *et al.* (2016) 'Expansion of Signal Transduction Pathways in Fungi by
608 Extensive Genome Duplication', *Current Biology*. doi: 10.1016/j.cub.2016.04.038.

609 Emms, D. M. and Kelly, S. (2018) 'OrthoFinder2: fast and accurate phylogenomic orthology
610 analysis from gene sequences', *bioRxiv*.

611 Giovannetti, M., Azzolini, D. and Citeresi, A. S. (1999) 'Anastomosis formation and nuclear
612 and protoplasmic exchange in arbuscular mycorrhizal fungi', *Applied and Environmental
613 Microbiology*. doi: 10.1128/aem.65.12.5571-5575.1999.

614 Gurevich, A. *et al.* (2013) 'QUAST: quality assessment tool for genome assemblies.',
615 *Bioinformatics (Oxford, England)*. doi: 10.1093/bioinformatics/btt086.

616 Hancock, John M. *et al.* (2004) 'HMMer', in *Dictionary of Bioinformatics and Computational*
617 *Biology*. doi: 10.1002/9780471650126.dob0323.pub2.

618 Heywood, J. L. *et al.* (2011) 'Capturing diversity of marine heterotrophic protists: One cell at a
619 time', *ISME Journal*. doi: 10.1038/ismej.2010.155.

620 Hibbett, D. S. *et al.* (2007) 'A higher-level phylogenetic classification of the Fungi',
621 *Mycological Research*. doi: 10.1016/j.mycres.2007.03.004.

622 Hoeksema, J. D. *et al.* (2018) 'Evolutionary history of plant hosts and fungal symbionts predicts
623 the strength of mycorrhizal mutualism', *Communications biology*. doi: 10.1038/s42003-018-
624 0120-9.

625 House, G. L. *et al.* (2016) 'Phylogenetically structured differences in rRNA gene sequence
626 variation among species of arbuscular mycorrhizal fungi and their implications for sequence
627 clustering', *Applied and Environmental Microbiology*. doi: 10.1128/AEM.00816-16.

628 Huson, D. H. and Bryant, D. (2006) 'Application of phylogenetic networks in evolutionary
629 studies', *Molecular Biology and Evolution*. doi: 10.1093/molbev/msj030.

630 James, T. Y. *et al.* (2006) 'Reconstructing the early evolution of Fungi using a six-gene
631 phylogeny', *Nature*. doi: 10.1038/nature05110.

632 James, T. Y. *et al.* (2020) 'Toward a Fully Resolved Fungal Tree of Life', *Annual Review of*
633 *Microbiology*. doi: 10.1146/annurev-micro-022020-051835.

634 Jany, J. L. and Pawlowska, T. E. (2010) 'Multinucleate spores contribute to evolutionary
635 longevity of asexual glomeromycota', *American Naturalist*. doi: 10.1086/650725.

636 Kalyaanamoorthy, S. *et al.* (2017) 'ModelFinder: Fast model selection for accurate phylogenetic
637 estimates', *Nature Methods*. doi: 10.1038/nmeth.4285.

638 Kameoka, H. *et al.* (2019) 'Stimulation of asymbiotic sporulation in arbuscular mycorrhizal
639 fungi by fatty acids', *Nature Microbiology*. doi: 10.1038/s41564-019-0485-7.

640 Kämper, J. *et al.* (2006) 'Insights from the genome of the biotrophic fungal plant pathogen
641 *Ustilago maydis*', *Nature*. doi: 10.1038/nature05248.

642 Katoh, K. (2002) 'MAFFT: a novel method for rapid multiple sequence alignment based on fast
643 Fourier transform', *Nucleic Acids Research*. doi: 10.1093/nar/gkf436.

644 Katoh, K. and Standley, D. M. (2013) 'MAFFT multiple sequence alignment software version 7:
645 Improvements in performance and usability', *Molecular Biology and Evolution*. doi:
646 10.1093/molbev/mst010.

647 Kobayashi, Y. *et al.* (2018) 'The genome of *Rhizophagus clarus* HR1 reveals a common genetic
648 basis for auxotrophy among arbuscular mycorrhizal fungi', *BMC Genomics*. doi:
649 10.1186/s12864-018-4853-0.

650 Köster, J. and Rahmann, S. (2012) 'Snakemake-a scalable bioinformatics workflow engine',

651 *Bioinformatics*. doi: 10.1093/bioinformatics/bts480.

652 Kozoli, L. *et al.* (2018) ‘The plant microbiome and native plant restoration: The example of
653 native mycorrhizal fungi’, *BioScience*. doi: 10.1093/biosci/biy125.

654 Krüger, M. *et al.* (2012) ‘Phylogenetic reference data for systematics and phylotaxonomy of
655 arbuscular mycorrhizal fungi from phylum to species level’, *New Phytologist*. doi:
656 10.1111/j.1469-8137.2011.03962.x.

657 De la Providencia, I. E. *et al.* (2013) ‘Detection of a transient mitochondrial DNA heteroplasmy
658 in the progeny of crossed genetically divergent isolates of arbuscular mycorrhizal fungi’, *New
659 Phytologist*. doi: 10.1111/nph.12372.

660 Lartillot, N., Lepage, T. and Blanquart, S. (2009) ‘PhyloBayes 3: A Bayesian software package
661 for phylogenetic reconstruction and molecular dating’, *Bioinformatics*. doi:
662 10.1093/bioinformatics/btp368.

663 Lebreton, A. *et al.* (2020) ‘Comparative genomics applied to Mucor species with different
664 lifestyles’, *BMC Genomics*. doi: 10.1186/s12864-019-6256-2.

665 Li, H. and Durbin, R. (2009) ‘Fast and accurate short read alignment with Burrows-Wheeler
666 transform’, *Bioinformatics*. doi: 10.1093/bioinformatics/btp324.

667 Li, L., Stoeckert, C. J. and Roos, D. S. (2003) ‘OrthoMCL: Identification of ortholog groups for
668 eukaryotic genomes’, *Genome Research*. doi: 10.1101/gr.1224503.

669 Li Y, Steenwyk JL, Chang Y, Wang Y, James TY, Stajich JE, Spatafora JW, Groenewald M,
670 Dunn CW, Hittinger CT, Shen X-X, Rokas A (2021) A genome-scale phylogeny of the kingdom
671 Fungi <https://doi.org/10.1016/j.cub.2021.01.074>

672 Lin, K. *et al.* (2014) ‘Single Nucleus Genome Sequencing Reveals High Similarity among
673 Nuclei of an Endomycorrhizal Fungus’, *PLoS Genetics*, 10(1). doi:
674 10.1371/journal.pgen.1004078.

675 Lofgren, L. A. *et al.* (2019) ‘Genome-based estimates of fungal rDNA copy number variation
676 across phylogenetic scales and ecological lifestyles’, *Molecular Ecology*. doi:
677 10.1111/mec.14995.

678 Ma, L. J. *et al.* (2009) ‘Genomic analysis of the basal lineage fungus *Rhizopus oryzae* reveals a
679 whole-genome duplication’, *PLoS Genetics*. doi: 10.1371/journal.pgen.1000549.

680 Maddison, W. and Knowles, L. (2006) ‘Inferring phylogeny despite incomplete lineage sorting’,
681 *Systematic Biology*. doi: 10.1080/10635150500354928.

682 Malar C, Mathu MC, Kruger M, Kruger C, Wang Y, Stajich JE, Keller J, Chen ECH, Yildirir G,
683 Villeneuve-Laroche M, Roux C, Delaux P-M, Corradi N (2021) The genome of *Geosiphon
684 pyriformis* reveals ancestral traits linked to the emergence of the arbuscular mycorrhizal
685 symbiosis. *Current Biology* <https://doi.org/10.1016/j.cub.2021.01.058>

686 Maeda, T. *et al.* (2018) 'Evidence of non-tandemly repeated rDNAs and their intragenomic
687 heterogeneity in *Rhizophagus irregularis*', *Communications Biology*. doi: 10.1038/s42003-018-
688 0094-7.

689 Marleau, J. *et al.* (2011) 'Spore development and nuclear inheritance in arbuscular mycorrhizal
690 fungi', *BMC Evolutionary Biology*. doi: 10.1186/1471-2148-11-51.

691 Martin, F. *et al.* (2008) 'The genome of *Laccaria bicolor* provides insights into mycorrhizal
692 symbiosis.', *Nature*, 452(7183), pp. 88–92. doi: 10.1038/nature06556.

693 Martin, F. *et al.* (2010) 'Périgord black truffle genome uncovers evolutionary origins and
694 mechanisms of symbiosis', *Nature*. doi: 10.1038/nature08867.

695 Martin, S. H. and Van Belleghem, S. M. (2017) 'Exploring evolutionary relationships across the
696 genome using topology weighting', *Genetics*. doi: 10.1534/genetics.116.194720.

697 Mirarab, S. and Warnow, T. (2015) 'ASTRAL-II: Coalescent-based species tree estimation with
698 many hundreds of taxa and thousands of genes', in *Bioinformatics*. doi:
699 10.1093/bioinformatics/btv234.

700 Mondo, S. J., Lastovetsky, O. A., *et al.* (2017) 'Bacterial endosymbionts influence host sexuality
701 and reveal reproductive genes of early divergent fungi', *Nature Communications*. doi:
702 10.1038/s41467-017-02052-8.

703 Mondo, S. J., Dannebaum, R. O., *et al.* (2017) 'Widespread adenine N6-methylation of active
704 genes in fungi', *Nature Genetics*. doi: 10.1038/ng.3859.

705 Montoliu-Nerin, M. *et al.* (2020) 'Building de novo reference genome assemblies of complex
706 eukaryotic microorganisms from single nuclei', *Scientific Reports*, 10(1), p. 1303. doi:
707 10.1038/s41598-020-58025-3.

708 Morin, E. *et al.* (2019) 'Comparative genomics of *Rhizophagus irregularis*, *R. cerebriforme*,
709 *R. diaphanus* and *Gigaspora rosea* highlights specific genetic features in Glomeromycotina',
710 *New Phytologist*. doi: 10.1111/nph.15687.

711 Muszewska, A. *et al.* (2017) 'Cut-and-paste transposons in fungi with diverse lifestyles',
712 *Genome Biology and Evolution*. doi: 10.1093/gbe/evx261.

713 Nguyen, L. T. *et al.* (2015) 'IQ-TREE: A fast and effective stochastic algorithm for estimating
714 maximum-likelihood phylogenies', *Molecular Biology and Evolution*. doi:
715 10.1093/molbev/msu300.

716 Novais, C. B. de *et al.* (2017) 'Compatibility and incompatibility in hyphal anastomosis of
717 arbuscular mycorrhizal fungi', *Scientia Agricola*. doi: 10.1590/1678-992x-2016-0243.

718 Okonechnikov, K., Conesa, A. and García-Alcalde, F. (2016) 'Qualimap 2: Advanced multi-
719 sample quality control for high-throughput sequencing data', *Bioinformatics*. doi:
720 10.1093/bioinformatics/btv566.

721 Parniske, M. (2008) 'Arbuscular mycorrhiza: The mother of plant root endosymbioses', *Nature Reviews Microbiology*. doi: 10.1038/nrmicro1987.

722 Pomraning, K. R. *et al.* (2018) ' Regulation of Yeast-to-Hyphae Transition in *Yarrowia* lipolytica ', *mSphere*. doi: 10.1128/msphere.00541-18.

723 Redecker, D. *et al.* (2013) 'An evidence-based consensus for the classification of arbuscular mycorrhizal fungi (Glomeromycota)', *Mycorrhiza*, 23(7), pp. 515–531. doi: 10.1007/s00572-013-0486-y.

724 Schluter, D. (2016) *Phylogenetic tools Phylogenetic trees*. Available at: <https://github.com/ballesterus/Utensils> (Accessed: 6 February 2020).

725 Schüßler, A. and Walker, C. (2010) 'The Glomeromycota. A species list with new families and new genera', *Schüßler A, Walker C, Gloucester, Published in libraries at Royal Botanic Garden Edinburgh, Kew, Botanische Staatssammlung Munich, and Oregon State University*, (December), p. 57. doi: 10.1097/MPA.0000000000000188.

726 Schüßler, A., Schwarzott, D. and Walker, C. (2001) 'A new fungal phylum, the Glomeromycota: phylogeny and evolution', *Mycological Research*, 105(12), pp. 1413–1421. doi: 10.1017/S0953756201005196.

727 Schwartz, V. U. *et al.* (2014) 'Gene Expansion Shapes Genome Architecture in the Human Pathogen *Lichtheimia corymbifera*: An Evolutionary Genomics Analysis in the Ancient Terrestrial Mucorales (Mucoromycotina)', *PLoS Genetics*. doi: 10.1371/journal.pgen.1004496.

728 Schwessinger, B. *et al.* (2018) 'A near-complete haplotype-phased genome of the dikaryotic wheat stripe rust fungus *Puccinia striiformis* f. sp. *tritici* reveals high interhaplotype diversity', *mBio*. doi: 10.1128/mBio.02275-17.

729 Simão, F. A. *et al.* (2015) 'BUSCO: Assessing genome assembly and annotation completeness with single-copy orthologs', *Bioinformatics*. doi: 10.1093/bioinformatics/btv351.

730 Smit, A. and Hubley, R. (2015) *RepeatModeler open-1.0*, Available at <http://www.repeatmasker.org>. doi: 10.1007/s00572-016-0720-5.

731 Smit, A., Hubley, R. and Green, P. (no date) 'RepeatMasker Open-4.0'. Available at: <http://www.repeatmasker.org>.

732 Smith, S. and Read, D. (2008) *Mycorrhizal Symbiosis, Mycorrhizal Symbiosis*. doi: 10.1016/B978-0-12-370526-6.X5001-6.

733 Spatafora, J. W. *et al.* (2016) 'A phylum-level phylogenetic classification of zygomycete fungi based on genome-scale data', *Mycologia*. doi: 10.3852/16-042.

734 Stamatakis, A. (2014) 'RAxML version 8: A tool for phylogenetic analysis and post-analysis of large phylogenies', *Bioinformatics*. doi: 10.1093/bioinformatics/btu033.

735 Stepanauskas, R. and Sieracki, M. E. (2007) 'Matching phylogeny and metabolism in the

756 uncultured marine bacteria, one cell at a time', *Proceedings of the National Academy of Sciences*
757 *of the United States of America*. doi: 10.1073/pnas.0700496104.

758 Stockinger, H., Walker, C. and Schüßler, A. (2009) "Glomus intraradices DAOM197198", a
759 model fungus in arbuscular mycorrhiza research, is not Glomus intraradices', *New Phytologist*.
760 doi: 10.1111/j.1469-8137.2009.02874.x.

761 Sun, X. *et al.* (2018) 'Genome and evolution of the arbuscular mycorrhizal fungus Diversispora
762 epigaea (formerly Glomus versiforme) and its bacterial endosymbionts', *New Phytologist*.
763 Wiley/Blackwell (10.1111), 0(0). doi: 10.1111/nph.15472.

764 Tang, N. *et al.* (2016) 'A Survey of the gene repertoire of Gigaspora rosea unravels conserved
765 features among glomeromycota for obligate biotrophy', *Frontiers in Microbiology*. doi:
766 10.3389/fmicb.2016.00233.

767 Tedersoo, L. *et al.* (2018) 'High-level classification of the Fungi and a tool for evolutionary
768 ecological analyses', *Fungal Diversity*. doi: 10.1007/s13225-018-0401-0.

769 Ter-Hovhannisyan, V. *et al.* (2008) 'Gene prediction in novel fungal genomes using an ab initio
770 algorithm with unsupervised training', *Genome Research*. doi: 10.1101/gr.081612.108.

771 Tisserant, E. *et al.* (2013) 'Genome of an arbuscular mycorrhizal fungus provides insight into the
772 oldest plant symbiosis', *Proceedings of the National Academy of Sciences*, 110(50), pp. 20117–
773 20122. doi: 10.1073/pnas.1313452110.

774 Uehling, J. *et al.* (2017) 'Comparative genomics of Mortierella elongata and its bacterial
775 endosymbiont Mycoavidus cysteinexigens', *Environmental Microbiology*. doi: 10.1111/1462-
776 2920.13669.

777 Vankuren, N. W. *et al.* (2013) 'Ribosomal RNA gene diversity, effective population size, and
778 evolutionary longevity in asexual Glomeromycota', *Evolution*, 67(1), pp. 207–224. doi:
779 10.1111/j.1558-5646.2012.01747.x.

780 Walker, A. W. *et al.* (2014) 'Phylogeny, culturing, and metagenomics of the human gut
781 microbiota', *Trends in Microbiology*. doi: 10.1016/j.tim.2014.03.001.

782 Wang, D. *et al.* (2013) 'Draft Genome Sequence of Rhizopus chinensis CCTCCM201021, Used
783 for Brewing Traditional Chinese Alcoholic Beverages', *Genome Announcements*. doi:
784 10.1128/genomea.00195-12.

785 White, M. M. *et al.* (2006) 'Phylogeny of the Zygomycota based on nuclear ribosomal sequence
786 data', *Mycologia*. doi: 10.3852/mycologia.98.6.872.

787 Wideman, J. G. *et al.* (2019) 'A single-cell genome reveals diplomonimidlike ancestry of
788 kinetoplastid mitochondrial gene structure', *Philosophical Transactions of the Royal Society B:
789 Biological Sciences*. doi: 10.1098/rstb.2019.0100.

790 Wijayawardene, N. N. *et al.* (2018) *Notes for genera: basal clades of Fungi (including*

791 *Aphidiomycota, Basidiobolomycota, Blastocladiomycota, Calcarisporiellomycota,*
792 *Caulochytriomycota, Chytridiomycota, Entomophthoromycota, Glomeromycota,*
793 *Kickxellomycota, Monoblepharomycota, Mortierellomyc*, *Fungal Diversity*. doi:
794 10.1007/s13225-018-0409-5 1.
795 Wood, V. *et al.* (2002) ‘The genome sequence of *Schizosaccharomyces pombe*’, *Nature*. doi:
796 10.1038/nature724.
797 Woyke, T. *et al.* (2009) ‘Assembling the marine metagenome, one cell at a time’, *PLoS ONE*.
798 doi: 10.1371/journal.pone.0005299.
799 Yoon, H. S. *et al.* (2011) ‘Single-cell genomics reveals organismal interactions in uncultivated
800 marine protists’, *Science*. doi: 10.1126/science.1203163.
801 Maarja Öpik, John Davison, Mari Moora, and Martin Zobel (2013) DNA-based detection and
802 identification of Glomeromycota: the virtual taxonomy of environmental sequences. *Botany*
803 <https://doi.org/10.1139/cjb-2013-0110>
804